

University at Albany, State University of New York

Scholars Archive

Biological Sciences

Honors College

Spring 5-2021

Loss of EAAC1 Decreases IPSC Amplitude at D1-D1 Medium Spiny Neuron Synapses

Ian Tschang

University at Albany, State University of New York, iantschang@gmail.com

The University at Albany community has made this article openly available.

Please share how this access benefits you.

Follow this and additional works at: https://scholarsarchive.library.albany.edu/honorscollege_biology

Recommended Citation

Tschang, Ian, "Loss of EAAC1 Decreases IPSC Amplitude at D1-D1 Medium Spiny Neuron Synapses" (2021). *Biological Sciences*. 72.

https://scholarsarchive.library.albany.edu/honorscollege_biology/72

This Honors Thesis is brought to you for free and open access by the Honors College at Scholars Archive. It has been accepted for inclusion in Biological Sciences by an authorized administrator of Scholars Archive. Please see [Terms of Use](#). For more information, please contact scholarsarchive@albany.edu.

Loss of EAAC1 Decreases IPSC Amplitude at D1-D1 Medium Spiny Neuron Synapses

An honors thesis presented to the
Department of Biology,
University at Albany, State University of New York
in partial fulfillment of the requirements
for graduation with Honors in Biology
and
graduation from The Honors College

Ian Tschang

Research Mentor: Annalisa Scimemi, Ph.D.

Second Reader: Robert Rosellini, Ph.D.

May 2021

Abstract

EAAC1 is a neuronal glutamate transporter expressed in the brain and the peripheral system, including kidney. Within the brain EAAC1 is mostly expressed in the cortex and striatum, two regions involved in the execution of stereotyped movements and reward-based behaviors. EAAC1 is expressed post-synaptically at excitatory synapses. By contrast, EAAC1 is expressed presynaptically at inhibitory synapses. Here, by transporting glutamate into the presynaptic terminal, EAAC1 supports GABA synthesis and release, as glutamate is a precursor for the biosynthesis of GABA. It is currently unknown whether EAAC1 is differentially expressed and whether it exerts a different modulatory effect at different types of GABAergic inhibitory synapses. The striatum contains two types of GABAergic long-range projection neurons, which receive dopaminergic inputs from the *substantia nigra pars compacta* (SNc) and *ventral tegmental area* (VTA). These neurons, called medium spiny neurons (MSNs) based on their morphology, can be distinguished based on immunohistochemical and anatomical criteria. The first group of neurons expresses D1 dopamine receptors; the second group expresses D2 dopamine receptors. D1-MSNs project to the SNc, whereas D2-MSNs project indirectly to the SNc via an intermediate synapse in the *globus pallidus*. Here we ask how EAAC1 modulates synaptic inhibition among D1-D1, D1-D2, D2-D1 and D2-D2 synapses. We first target the expression of the light-gated ion channel Channelrhodopsin-2 (ChR2) to D1- or D2-MSNs by taking advantage of the Cre-LoxP system using BAC transgenic mice. We then use a fluorescence *in situ* hybridization (FISH) approach to determine whether EAAC1 is differentially expressed in D1- and D2-MSNs. Our data show that there is a preferential effect of EAAC1 at D1-D1 synapses as opposed to D1-D2, D2-D1, and D2-D2 synapses, and that this preferential effect may be due to an increased concentration of EAAC1 in D1-MSNs. These findings shed light on the interplay of neuronal circuits in the striatum, and may better our understanding of neuropsychiatric disorders such as OCD.

Keywords: *EAAC1, OCD, GABA, Glutamate, Neuropsychiatric disorders*

Acknowledgements

First and foremost, I would like to thank my PI Dr. Annalisa Scimemi for all the teaching and support during my years in the lab and while writing this thesis. I would also like to thank Maurice Petroccione and Nurat Affinnih, who have worked tirelessly on this project and helped to instruct me on the many techniques that were used, especially stereotaxic surgeries. A special thanks to Gabrielle Todd, who has kept our lab organized and efficient, whether it be in supplying mice or guidance in general. Thank you to Dr. Robert Rosellini, for serving as my second reader in this thesis and for counsel and direction. I would also like to thank my friends and family for the emotional support during my writing of this thesis. This work was supported by NSF grants IOS1655365 and IOS2011998.

List of Figures

Figure 1 TBOA reduces the mIPSC amplitude in D1-, but not D2-MSNs in WT mice.....	11
Figure 2 TBOA does not reduce the mIPSC amplitude in D1- and D2-MSNs in EAAC1 ^{-/-} mice	12
Figure 3 Stereotaxic injections of dLight1.3b into the DLS	13
Figure 4 IPSC amplitude decreased at D1-D1 synapses in EAAC1 ^{-/-} mice	15
Figure 5 D1-MSNs in WT mice are most susceptible to GABAergic modulation by D1-MSNs	16
Figure 6 RNAscope FISH for D1, D2, and EAAC1	16
Figure 7 RNAscope FISH PCA	17

Table of Contents

Abstract	ii
Acknowledgements	iii
List of Figures	iv
Introduction	1
Materials and Methods	4
Ethics Statement.....	4
Mice	4
Stereotaxic Surgery.....	5
Trans-cardial Perfusion and Section Preparation.....	6
ChR2 Stimulation and Electrophysiology Recordings	7
RNAscope FISH	7
Results	10
TBOA reduces mIPSC amplitude in D1-, not D2-MSNs.....	10
TBOA does not reduce the amplitude of mIPSCs in EAAC1-/- D1- and D2-MSNs.....	11
The absence of EAAC1 decreases evoked IPSC amplitude at D1-D1 connections	13
D1-MSNs in WT mice are most susceptible to GABAergic modulation by D1-MSNs	16
Visualization of the mRNA encoding EAAC1, D1 and D2 receptors using RNAscope	16
Discussion and Conclusions	18
References	21

Introduction

The Excitatory Amino Acid Carrier 1 (EAAC1) is a neuronal glutamate transporter that is most highly expressed in the cortex, hippocampus, and dorsal striatum in the brain (Rothstein et al., 1994). By rapidly binding and slowly transporting glutamate into neurons, EAAC1 lowers the glutamate concentration as it diffuses out of the synaptic cleft. EAAC1 is expressed in axons of GABAergic neurons and dendrites of glutamatergic neurons. Therefore, it is expressed presynaptically in inhibitory neurons and postsynaptically in excitatory neurons (He et al., 2000).

Previous work in the hippocampus showed that EAAC1 prolongs the clearance of glutamate from the synaptic cleft by astrocytes in the CA1 region of the hippocampus by serving as a glutamate buffer, a phenomenon that in turn can influence glutamate receptor activation. By rapid binding and slowly releasing glutamate in the extracellular space, EAAC1 reduces the activation of a particular class of glutamate receptors – the NMDA receptors – with high affinity for glutamate (Scimemi et al., 2009). In the striatum, limits the activation of a distinct class of glutamate receptors – the mGluRI – receptors, which are metabotropic glutamate receptors. Activation of mGluRI in mice expressing EAAC1 and D1 dopamine receptor (D1R) leads to a decrease in trafficking of D1R to the plasma membrane and an increase in repeated movements, while blocking mGluRI in EAAC1^{-/-} mice restored the WT phenotype: an increase in synaptic plasticity and D1R expression (Bellini et al., 2018).

At inhibitory terminals, EAAC1 serves to supply the terminal with glutamate, which can be used as a precursor for the biosynthesis of GABA. Consistent with this, previous studies have shown that raising extracellular glutamate levels increased mIPSC amplitude due to the increase in glutamate uptake and GABA production (Matthews & Diamond, 2003). When you use the in-text citation in Conversely, blocking glutamate transporters reduced mIPSC amplitude (Matthews

& Diamond, 2003). Here, we ask whether EAAC1 exerts a similar role at inhibitory synapses in the striatum.

The striatum is region of the brain responsible for inputting information into the basal ganglia and has been shown to be necessary for movement control. It consists of the caudate, putamen, and ventral striatum, which contains the *nucleus accumbens* (NAcc) (Báez-Mendoza & Schultz, 2013). The two main long-range projections from the striatum are formed by the axons of D1R- or D2R-expressing MSNs. D1-MSNs form the direct pathway and target the SNc. D2-MSNs form the indirect pathway and target the globus pallidus. Neurons of the D2 pathway (increase firing of GABAergic neurons in the basal ganglia, inhibiting downstream activity and suppressing movement (Freeze et al., 2013). The direct pathway begins in the cortex and projects to the striatum, continuing to the globus pallidus/substantia nigra and finally the thalamus. The indirect pathway begins similarly to the direct pathway, projecting from the cortex to the striatum. From the striatum, the indirect pathway continues to the external globus pallidus, and then on to the subthalamic nucleus (instead of directly to the thalamus). From there, the indirect pathway projects to the globus pallidus/substantia nigra and then continues with the direct pathway to the thalamus (Young et al., 2020).

The inhibitory relationship between D1- and D2-MSNs, is still unclear. Here, we use ChR2, a light-gated cation channel that leads to photocurrents in stimulated neurons (Nagel et al., 2003), to initiate post synaptic currents and record effects on D1 and D2-MSNs and the effect of EAAC1. We stereotaxically injected the viral construct containing floxed ChR2 (DNA flanked on both sides by LoxP sites) into the striatum of P12-P18 mice and used the Cre-LoxP system to integrate the construct into the host genome. This system works through the expression of Cre-recombinase, which recognizes and recombines DNA at LoxP sites (Kim et al., 2018), effectively inserting ChR2

into the genome of the mouse. We then use RNAscope Fluorescence *In Situ* Hybridization (FISH) technology (Wang et al., 2012), which uses hybridization of Z-shaped probes and amplification to determine the expression level of the mRNA encoding EAAC1, D1 and D2 receptors. A principal component analysis (PCA) can help us to see differences in gene expression between D1- and D2-MSNs.

Our findings may have implications in Obsessive-compulsive disorder (OCD), since several candidate genes have been identified to contribute to OCD, including *DLGAP1*, *PTRD*, and *SLCIA1*, which is the gene that encodes EAAC1 (Purty et al., 2019). OCD is a mental illness that is highly characterized by persistent, intrusive thoughts and stereotyped behaviors. It has been known to cause certain individuals to spend hours of the day performing washing and checking rituals. Around 2-3% of the world's population has been diagnosed with OCD and the mean age of onset ranges from 22-36 years of age (Jenicke, 2004). *SLCIA1* has been proven to be a promising candidate gene for the diagnosis and treatment of OCD (Samuels et al., 2011). However, our understanding of gene expression and interaction is still largely unclear, and it is most likely that the genetic basis of OCD is extremely complex.

Materials and Methods

Ethics Statement

All experimental procedures were performed in accordance with protocols approved by the Institutional Animal Care and Use Committee at the State University of New York (SUNY) Albany and guidelines described in the National Institutes of Health's Guide for the Care and Use of Laboratory Animals.

Mice

All mice were group housed and kept under a 12 h light cycle (7:00 A.M. on, 7:00 P.M. off) with food and water available. Constitutive EAAC1 knockout mice (EAAC1^{-/-}) were obtained by targeted disruption of the *Slc1a1* gene via insertion of a *pgk* neomycin resistance cassette in exon 1 of the *Slc1a1* gene. EAAC1^{-/-} breeders were generated after back-crossing EAAC1^{+/-} mice with C57BL/6 mice for more than 10 generations. C57BL/6 mice were identified as EAAC1 WT or EAAC1^{-/-} at postnatal day 0 (P0) to P35 using PCR analysis of genomic DNA. EAAC1^{-/-} mice develop normally during the first 5 weeks of postnatal life. They are fertile and, although they give birth to smaller litters, the litters are as viable as those of WT mice and have a similar sex distribution. D1^{Cre/+} mice and A2A^{Cre/+} mice were kindly provided by Drs. A.V. Kravitz and C.F. Gerfen (National Institute of Diabetes and Digestive and Kidney Diseases –National Institutes of Health). In these mice, the protein Cre-recombinase is expressed under the control of the promoter for D1s and the adenosine receptor 2, which co-localizes with D2 dopamine receptors (D2Rs), respectively. Genotyping was performed on toe tissue samples of P7–P10 mice. Briefly, tissue samples were digested at 55°C overnight in a lysis buffer containing the following (in mM): 100

Tris base, pH 8, 5 EDTA, and 200 NaCl, along with 0.2% SDS and 100 µg/ml proteinase K. DNA samples were diluted in nuclease-free water (500 ng/µl) and processed for PCR analysis. The PCR primers used for EAAC1, D1^{Cre/+}, and A2A^{Cre/+} were purchased from Fisher Scientific. The PCR protocol for EAAC1, D1^{Cre/+}, and A2A^{Cre/+} were performed using standard TaqDNA Polymerase (catalog #R2523; Millipore Sigma).

Stereotaxic Surgeries

Bilateral stereotaxic injections of AAV5-DIO-Ef1A-hChR2-(H134R)-DYFP-WPRE-PA in the dorsolateral striatum (DLS) were performed on mice of either sex aged P12-18. The mouse strains used for these procedures included: D1^{Cre/+}, A2A^{Cre/+}, D1^{Cre/+}: EAAC1^{-/-} and A2A^{Cre/+}: EAAC1^{-/-}. To perform the stereotaxic surgeries, we first monitored the mouse weight to be able to exclude any runt pup (<6 g at P14-18). We then placed the mouse in an induction chamber and administered 5% isoflurane. We then removed the fur on the top of the head with a hair remover lotion (such as Nair) and the mouse was positioned into the microinjection stereotaxic frame (Neurostar) on a hand warmer to prevent an unsustainable drop in body temperature. In the frame, the mouse received a continuous dosage of 2-3% isoflurane. Lidocaine was applied to the scalp for two minutes to allow for proper anaesthetization. The scalp was then cleaned with three alternating applications of betadine and 70% ethanol. Artificial tears were applied to the eyes to prevent drying. A tail pinch was used to determine the depth of the anesthesia and if no reaction was observed, we proceeded with the surgery. A midsagittal incision was made in the scalp and bregma, the point where the frontal and the two parietal bones fuse, was located and was used as a point of reference for the injection. The coordinates of the DLS are AP: +0.2 mm, ML: ±2.0 mm; DV: -2.8 mm. We use a drill to thin the skull in the area of interest. A Hamilton syringe was used

to inject 0.2 μ l of the construct at a rate of 0.05 μ l/min. After injection has finished, we waited one minute before retracting the needle halfway, and then another 30 s before retracting the needle fully out of the brain. This is to ensure proper diffusion of the viral construct. Injections were done bilaterally in the DLS. The incision site was closed with surgical glue and lidocaine is applied once again, along with an antibiotic ointment. A subcutaneous injection of a 10% v/w saline was performed to rehydrate the mouse. The mouse was then placed in the recovery cage on another hand warmer separate from the mother to properly recover from anesthesia and surgery. Body weight, behavior, site of incision and overall well-being of the mouse was monitored over the next 72 hr.

Trans-cardial Perfusion and Section Preparation

We performed trans-cardial perfusion of the mice used for the stereotaxic surgeries 3-4 weeks after the surgery, to allow for ChR2 expression. The mice were deeply anesthetized using halothane, which was dabbed onto a cotton ball and placed over the head of the mouse and trans-cardially perfused with 10 ml of sucrose ACSF slicing solution. The mouse was then decapitated in accordance with SUNY–Albany Animal Care and Use Committee guidelines. The brain was rapidly removed and placed in ice-cold slicing solution bubbled with 95% O₂/5% CO₂ containing the following (in mM): 119 NaCl, 2.5 KCl, 0.5 CaCl₂, 1.3 MgSO₄·H₂O, 4 MgCl₂, 26.2 NaHCO₃, 1 NaH₂PO₄, and 22 glucose, 320 mOsm, pH 7.4. Coronal slices (250 μ m thick) were prepared using a vibrating blade microtome (VT1200S; Leica Microsystems). Once prepared, the slices were stored in this solution in a submersion chamber at 36°C for 30 min and at RT for at least 30 min and up to 5 h. The recording solution contained the following (in mm): 119 NaCl, 2.5 KCl, 1.2 CaCl₂, 1 MgCl₂, 26.2 NaHCO₃, and 1 NaH₂PO₄, 22 glucose, 300 mOsm, pH 7.4. This solution

was also used to fill the glass capillaries used for extracellular field recordings. We identified the DLS under bright-field illumination using an upright fixed-stage microscope (BX51 WI; Olympus).

ChR2 Stimulation and Electrophysiology Recordings

Stimulating and recording electrodes were both placed in the DLS ~ 100 μm away from each other. We delivered white light through the epifluorescence port of an upright microscope and passed it through an FITC filter set to activate ChR2 and evoke postsynaptic responses. Each light pulse was 5 ms long and was delivered every 30 s. The resistance of the recording electrode was ~ 1.5 $\text{M}\Omega$ and was monitored throughout the experiments. Data were discarded if the resistance changed $>20\%$ throughout the course of the experiment. We recorded IPSCs in the presence of the AMPA receptor antagonist (NBQX, 10 μM) and the NMDA receptor antagonist (APV, 50 μM), at a holding potential of 0 mV. D,L-threo- β -Benzyloxyaspartic acid (TBOA) was used to block glutamate receptors (including EAAC1) and recordings were performed in acute striatal slices from EAAC1^{-/-} and WT mice expressing both D1^{Cre/+} and A2A^{Cre/+}. All recordings were obtained using a Multiclamp 700B amplifier and filtered at 10 kHz (Molecular Devices), converted with an 18-bit 200 kHz A/D board (HEKA), digitized at 10 kHz, and analyzed offline with custom-made software (A.S.) written in IgorPro 6.36 (Wavemetrics). All recordings were performed at RT.

RNAscope FISH

We dissected the mice, removed the brain, and placed it into a slicing solution (119 mM NaCl, 2.5 mM KCl, 0.5 mM CaCl₂, 1.3 mM MgSO₄_H₂O, 4 mM MgCl₂, 26.2 mM NaHCO₃, 1

mM NaH₂PO₄, and 22 mM glucose, 320 mOsm, pH7.4) bubbling with 95% O₂, 5% CO₂. We fixed the whole brain in 4% PFA in 1X PBS for 24 hr at 4°C overnight. After washing carefully in 1X PBS, 5 times, 30 min each, we cryoprotected the brain in 30% sucrose in 1X PBS until the brain sinks. After washing carefully in 1X PBS, 5 times, 30 min each we prepared sagittal slices 30 μm thick with a vibrating blade microtome. We then incubated the slices in 4% PFA in PBS overnight to post-fix. We permeabilized the slices by soaking them in 0.5X TBS + 0.1% Tween 20 (0.5X TBST) overnight at 4°C (or up to two days at 4°C). We mounted the slices on Superfrost Plus slides after washing them in 0.5X TBST once and allowed them to dry for 1 hour at RT. We then dipped the slides in water 3X for less than 3 s each and once again allowed them to air dry at RT for 1 hr. The slides were then baked for 1 hr at 60°C and then incubated at RT for 2 hr in 4% PFA in 1X PBS. We dehydrated the slides using an ethanol gradient (50, 70, 100%) for 10-15 min each and dried them for 15 min at 60°C. We used the following procedure to block endogenous peroxidase enzyme activity to prevent hazy background after detection: Incubate slides for 10 min in hydrogen peroxide at RT, rinse the slide carefully with water and allow to air dry for 20 min at RT to prevent slices from curling, dry the slide for 15 min at 60°C. We then carried out a target retrieval and removed the crosslinking introduced by the fixative: cover slides with foil and bring to a boil on a heat block, perform the target retrieval with dilute 1X Target Retrieval buffer in water (from 10X stock) for 10 min at 100°C, rinse slides with water and then 100% ethanol, allow to air dry at RT to prevent slices from curling, dry the slides for 10 min at 60°C. A protease treatment was then performed to permeabilize the cell and allow the probe to enter: draw a hydrophobic barrier around the slices on the slide with a hydrophobic marker, prepare the humidity control chamber, add 150 μl drops of Protease III to slides and digest for 30 min at 40°C, rinse with twice with distilled water. We hybridized probes C1, C2, and C3, which hybridize to D1R,

SLC1A1, and D2R, respectively, by placing the slides in a humidity control chamber and adding about 150 μ l of probe per slice. We allowed the probes to hybridize for 2 hr at 40°C and then washed the slides in 1X Wash buffer for 2 min at RT twice. We then hybridized the amplifiers (AMP 1, AMP 2, and AMP3): add 150 μ l of RNAscope multiplex FL v2 AMP 1 to completely cover the slide and incubate for 30 min at 40°C in the humidity control chamber; wash slides in 1X Wash buffer for 2 min at RT twice; repeat step for AMP 2 and AMP3.

After the hybridization and amplification is complete, we added fluorophores to the slices. To develop the HRP-C1 signal, we added 150 μ l of RNAscope Multiplex FL v2 HRP-C1 to fully cover the slide, incubated for 15 min at 40°C in the humidity control chamber, and washed slides in 1X Wash buffer for 2 min at RT twice. After removing excess liquid, we added 150 μ l of diluted Opal 520 (fluorophore) to each slide and incubated for 30 min at 40°C on the rack in the humidity control chamber and washed slides in 1X Wash buffer for 2 min at RT twice. Once again, we removed excess liquid and then added 150 μ l of RNAscope Multiplex FL v2 HRP blocker to fully cover each slide, incubated for 15 min at 40°C in the humidity control chamber and performed two more 1X Wash buffer washes. We carried out the same procedure to develop the HRP-C2 signal (using Opal 570) and HRP-C3 (using Opal 690). After RNAscope was completed, we counter stained the slices with DAPI, mounted them on Superfrost Plus slides, then obtained images using a confocal microscope. All reagents for RNAscope FISH were purchased from Advanced Cell Diagnostics, Inc.

Results

TBOA reduces mIPSC amplitude in D1-, not D2-MSNs

In a first set of experiments, we asked how blocking glutamate transporters changed the amplitude and kinetics of GABAergic synaptic currents evoked by different sets of inhibitory inputs, coming from either D1- or D2-MSNs. The experimental design was based on the following rationale. Electron microscopy studies show that EAAC1 is expressed presynaptically at GABAergic synapses (He et al, 2000). If EAAC1, by taking up glutamate from the extracellular space, contributes to GABA synthesis and release, then blocking all glutamate transporters should have a different effect in WT and EAAC1^{-/-} mice. Differences in effects at D1 and D2 connections may indicate differences in concentration of EAAC1 at these synapses, or differences in their probability of being activated, which could also be attributed to differences in their local density of expression along the plasma membrane.

The addition of TBOA, which blocks glutamate transporters including but not limited to EAAC1, led to a decrease in the amplitude of miniature Inhibitory Post Synaptic Currents (mIPSCs) in D1-MSNs (**Figure 1A**). Despite a decrease in amplitude of mIPSCs, we did not detect a decrease in rise or decay time (t_{50} is the time it takes for the current to decay to 50% of its peak; **Figures 1B & 1C**). D2-MSNs experienced mIPSCs that were almost identical to the control when TBOA was added (**Figure 1D**), showing no significance in amplitude, rise time, and t_{50} (**Figures 1E & 1F**). TBOA has a greater effect on the mIPSC amplitude of D1-MSNs, but does not have a significant effect on the amplitude of mIPSCs in D2-MSNs. TBOA also does not have a significant effect on rise time and t_{50} of both D1- and D2-MSNs.

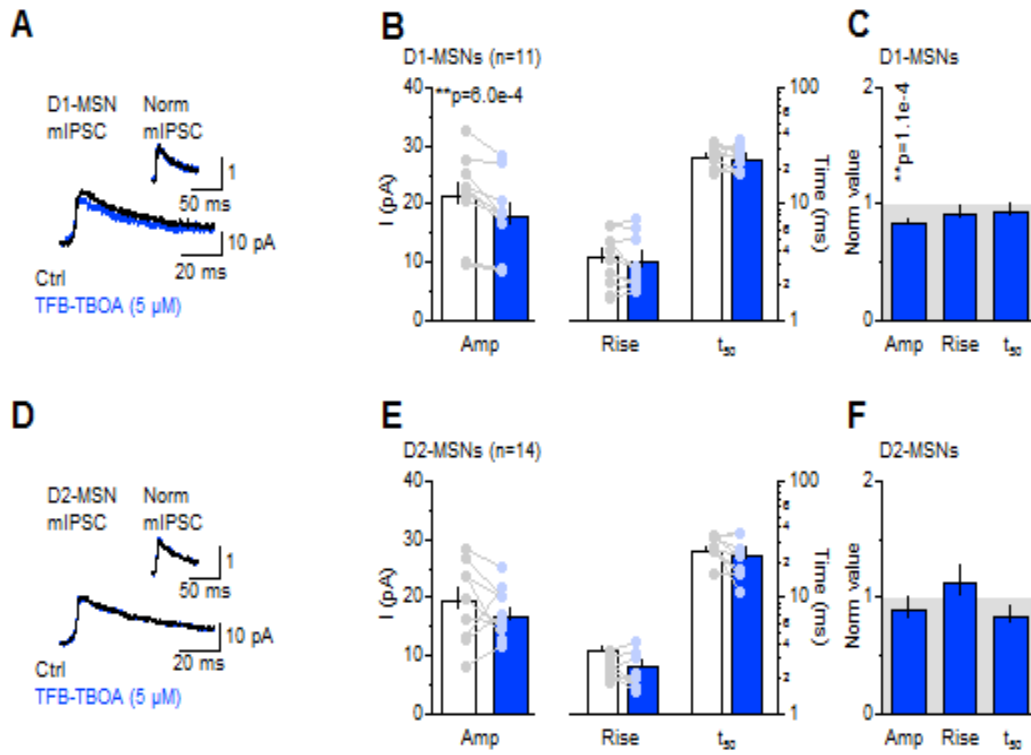


Figure 1 TBOA reduces the mIPSC amplitude in D1-, but not D2-MSNs in WT mice

A) Electrophysiological recordings in WT D1-MSNs, showing mIPSCs in control and preparations where TBOA was added. B) Bar graph of amplitude, rise time, and t_{50} of mIPSCs in D1-MSNs. TFB-TBOA decreased the mIPSC amplitude, but not rise time and t_{50} . C) Amplitude, rise time, and t_{50} of D1-MSNs when TBOA was added, as compared to control (indicated by grey shading). D) Electrophysiological recordings in WT D2-MSNs, showing mIPSCs in control and preparations where TBOA was added. E) Bar graph of amplitude, rise time, and t_{50} of mIPSCs in D2-MSNs. No significance in amplitude, rise time, or t_{50} was observed. F) Amplitude, rise time, and t_{50} of D2-MSNs when TBOA was added, as compared to control (indicated by grey shading).

TBOA does not reduce the amplitude of mIPSCs in EAAC1^{-/-} D1- and D2-MSNs

TBOA did not change the mIPSC amplitude, rise time and t_{50} in D1-MSNs of EAAC1^{-/-} mice (Figure 2A, 2B, & 2C). Similar results were obtained in D2-MSNs of EAAC1^{-/-} mice (Figure 2D, 2E, & 2F). This suggests that the larger effect of TBOA on D1-MSNs in WT mice is due to EAAC1, not other glutamate transporters. Note that all these mIPSC recordings were

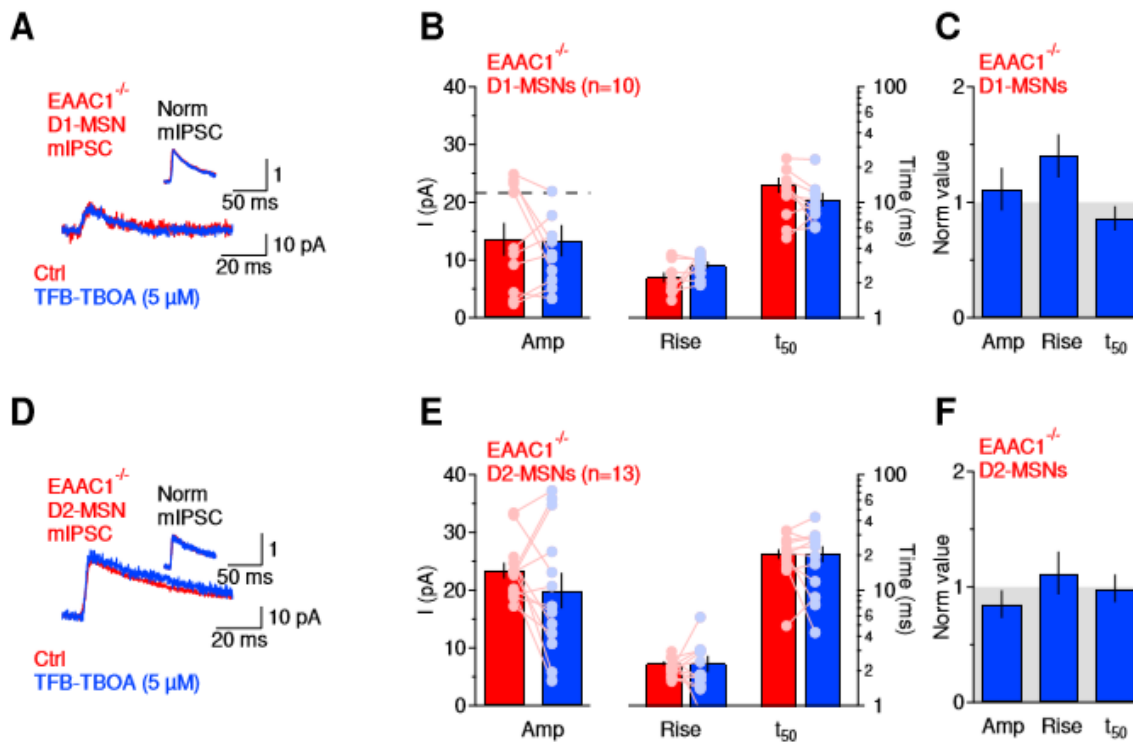


Figure 2 TBOA does not reduce the mIPSC amplitude in D1- and D2-MSNs in EAAC1^{-/-} mice

A) Electrophysiological recordings in D1-MSNs of EAAC1^{-/-} mice, showing mIPSCs in control and preparations where TBOA was added. B) Bar graph of amplitude, rise time, and t₅₀ of mIPSCs in D1-MSNs. We detected no significance in amplitude, rise time, or t₅₀. C) Summary of the effect of TBOA on the IPSC amplitude, rise time, and t₅₀, as compared to control (indicated by grey shading). D) Electrophysiological recordings in EAAC1^{-/-} D2-MSNs, showing mIPSCs in control and preparations where TBOA was added. E) Bar graph of amplitude, rise time, and t₅₀ of mIPSCs in D2-MSNs. No significance in amplitude, rise time, or t₅₀ was observed. F) Amplitude, rise time, and t₅₀ of D2-MSNs when TBOA was added, as compared to control (indicated by grey shading).

performed by holding the cells we patched at 0 mV. This depolarized potential prevents postsynaptic glutamate uptake. Therefore, the effect of TBOA on D1-MSN from WT mice is presynaptic and not postsynaptic.

The absence of EAAC1 decreases evoked IPSC amplitude at D1-D1 connections

By injecting an adeno-associated virus (AAV) containing Chr2, we achieved effective transfection into the dorsolateral striatum of WT and EAAC1^{-/-} mice (**Figure 3**). We recorded from D1-MSNs in WT and EAAC1^{-/-} mice that were transfected with Chr2 into D1-MSNs in the striatum by way of D1^{Cre/+} (**Figure 4A**). When TBOA was applied to this preparation, a decrease in IPSC amplitude was observed (**Figure 4E**, top trace). We did the same recordings for EAAC1^{-/-} mice and saw that the application of TBOA did not affect the amplitude of IPSCs (**Figure 4E**, bottom trace). However, EAAC1^{-/-} mice displayed significantly decreased IPSC amplitude when compared to EAAC1 WT mice in D1-D1 connections (**Figure 4E**, graph). TBOA had a much greater effect on the amplitude of IPSCs in D1-D1 connections of WT mice than on EAAC1^{-/-} mice (**Figure 4I**). We expect to see a greater effect of TBOA in WT mice than in EAAC1^{-/-} mice due to the presence of EAAC1 glutamate transporters, in addition to GLAST and GLT-1. D1-D1 connections appear to be strongly modulated by EAAC1.

We also recorded from D1-MSNs in WT and EAAC1^{-/-} mice that were transfected with Chr2 into D2-MSNs (**Figure 4B**). We did not see a significant decrease in IPSC amplitude when TBOA was applied in both WT and EAAC1^{-/-} mice (**Figure 4F**), and there were not significant decreases when EAAC1^{-/-} mice were compared to WT mice in D2-D1 connections (**Figure 4J**). D1-D2 inhibitory connections were also explored in WT and EAAC1^{-/-} mice (**Figure 4C**). We did

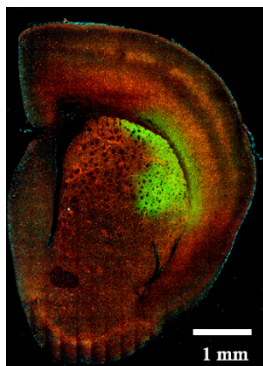


Figure 3. Stereotaxic injections of dLight1.3b into the DLS

By injecting an AAV containing Chr2 conjugated with an EYFP fluorophore, we achieve effective transfection into the striatum (shown in green). Transfection in this image is in a D1-tdTomato mouse (red fluorescence).

not see a significant decrease in IPSC amplitude when TBOA was applied in both WT and EAAC1^{-/-} mice (**Figure 4G**), and there were not significant decreases when EAAC1^{-/-} mice were compared to WT mice in D1-D2 synapses

(**Figure 4L**). In D2-D2 synapses (**Figure 4D**), we also did not see a significant decrease in IPSC amplitude when TBOA was applied in both WT and EAAC1^{-/-} mice (**Figure 4H**), and there were not significant decreases when EAAC1^{-/-} mice were compared to WT mice in D2-D1 connections (**Figure 4M**). What is surprising about these data is that the modulation by EAAC1, as seen in a significant decrease in IPSC amplitude with the addition of TBOA, is only apparent at D1-D1 connections and is absent at all other synaptic connections between D1 and D2-MSNs.

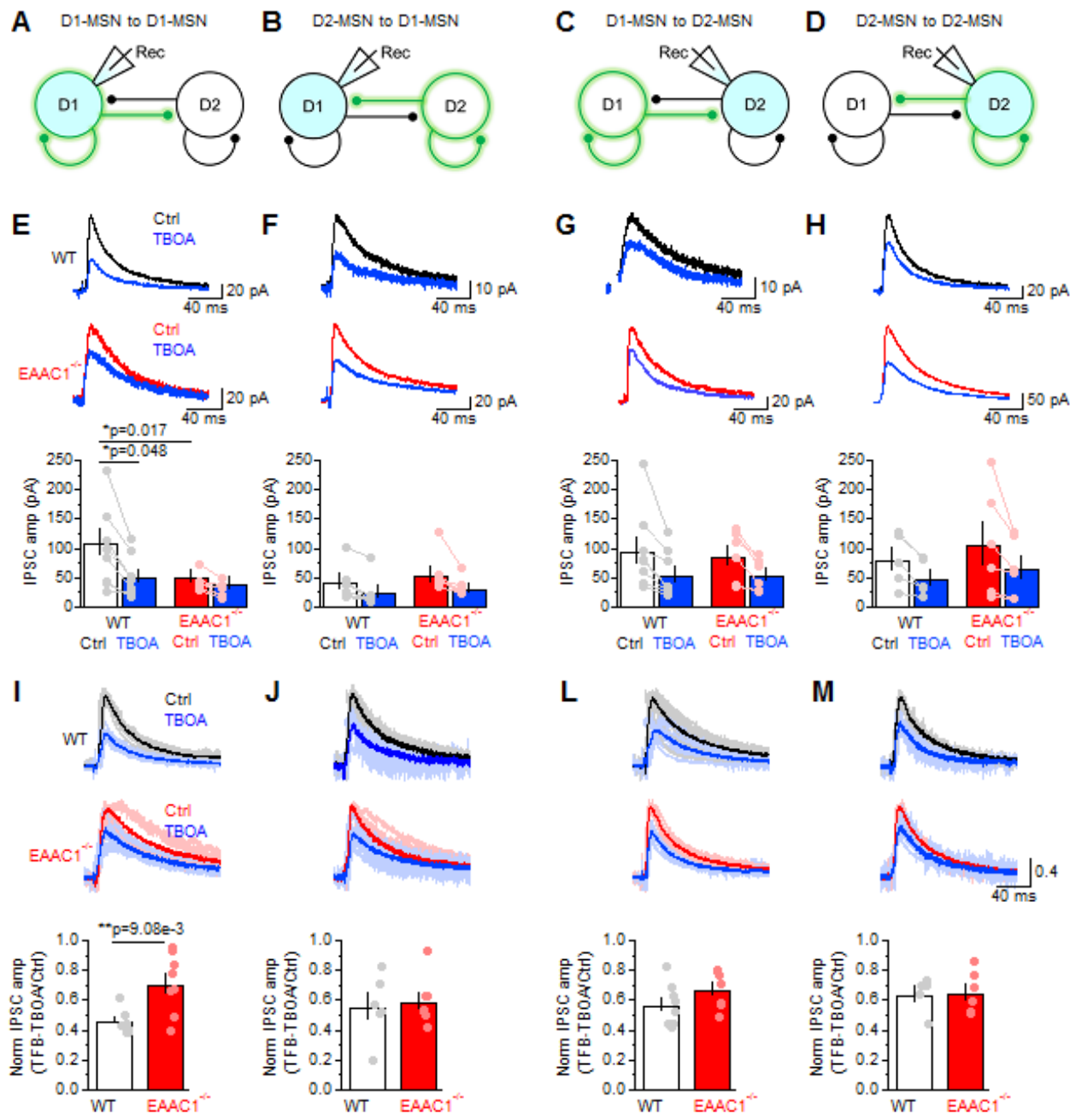


Figure 4 IPSC amplitude decreased at D1-D1 synapses in EAAC1^{-/-} mice

A)-D) Schematic of electrophysiological recordings (e.g. A) shows that D1-MSNs were stimulated and D1-MSNs were recorded from) E)-H) Electrophysiological recordings of evoked IPSCs in EAAC1 WT mice when TBOA was added (top trace) and EAAC1^{-/-} mice when TBOA was added (bottom trace) as compared to control. EAAC1^{-/-} mice experienced a decrease in IPSC amplitude when compared to WT mice in D1-D1 connections. I)-M) Traces of evoked IPSCs in WT and EAAC1^{-/-} mice in the presence and absence of TBOA (top) and graph of amplitude when TBOA was added compared to control (Y-axis is normalized IPSC amplitude: TBOA amplitude divided by control amplitude). TBOA had a much greater effect on the amplitude of IPSCs in D1-D1 connections of WT mice than on EAAC1^{-/-} mice.

D1-MSNs in WT mice are most susceptible to GABAergic modulation by D1-MSNs

D1-MSNs in WT mice saw greater inhibitory modulation by D2-, but mainly D1-MSNs (44% and 53%, respectively), as compared to inhibition coming from other sources. D2-MSNs in WT mice as well as both D1- and D2-MSNs in EAAC1^{-/-} mice saw a relatively even amount of inhibition coming from D1-MSNs, D2-MSNs and other sources (**Figure 5**).

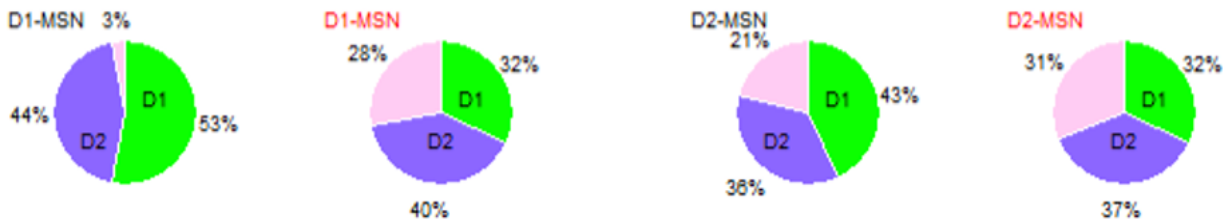


Figure 5 D1-MSNs in WT mice are most susceptible to GABAergic modulation by D1-MSNs

Amount of reduction in IPSCs when provided by D1-MSNs (green), D2-MSNs (blue), or other (pink) for D1 and D2-MSNs of WT (black label) and EAAC1^{-/-} mice (red label). D1-MSNs in WT mice saw greater inhibitory modulation by D2, but mainly D1-MSNs, as compared to inhibition coming from other sources.

Visualization of the mRNA encoding EAAC1, D1 and D2 receptors using RNAscope

In another experiment, we carried out an RNAscope to measure D1 and D2 dopamine receptors and EAAC1 mRNA expression levels. We asked whether the differential effect of EAAC1 at D1-D1 synapses may be due to differential expression of EAAC1 at these synapses.

Figure 6 shows a representative image of one such slice that we obtained from RNAscope FISH.

It shows neuronal somas stained by DAPI as well as puncta of distinct colors, mostly contained

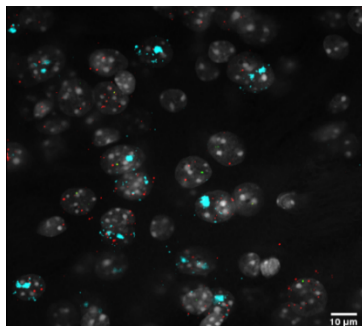


Figure 6 RNAscope FISH for D1, D2, and EAAC1

A representative confocal image of a slice after hybridization of RNAscope probes and Opal dyes. Green puncta represent D1 dopamine receptors, cyan puncta represent D2 receptors, red puncta represent *SLC1A1* mRNA (encoding the glutamate transporter EAAC1), and DAPI staining is shown in grey to visualize neuronal somas.

within each soma, representing D1 receptors (*green*), D2 receptors (*cyan*), and EAAC1 (*red*).

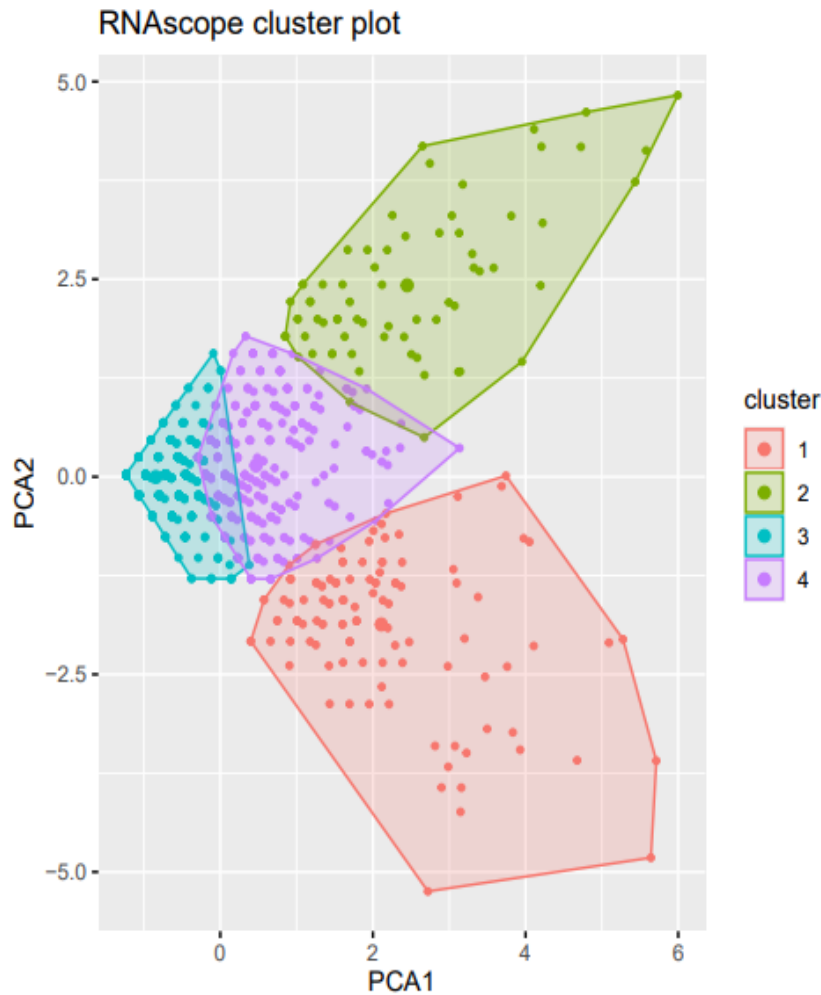


Figure 7 RNAscope FISH PCA

Four distinct clusters are shown in the figure: one expressing D1 dopamine receptors and EAAC1 (cluster 1, red), one that expressed primarily D2 receptors and EAAC1 (cluster 2, green), one that expressed none of them (cluster 3, blue), and one that expressed all three mRNAs (cluster 4, purple). The size calculations are as follows: cluster 1 – 114, cluster 2 – 69, cluster 3 – 670, and cluster 4 – 334.

receptors and EAAC1 (cluster 1, size 114) was almost double the size of the cluster that expressed D2 receptors and EAAC1 (cluster 2, size 69). This reveals that EAAC1 is more concentrated at D1-D1 synapses, which may be why we see a preferential inhibitory effect of EAAC1 at D1-D1 synapses. However, most MSNs fall into clusters that expressed none of the mRNAs (cluster 3, size 670) and all three mRNAs (cluster 4, size 334).

We used a novel software encoded in R to quantify the number of D1, D2, and EAAC1 mRNA in all the images that we obtained.

We then carried out a PCA and found four distinct groups of MSNs: one that expressed primarily D1 receptors and EAAC1, one that expressed primarily D2 receptors and EAAC1, one that expressed none of them, and one that expressed all three mRNAs

(Figure 7). We found that the size of the cluster for MSNs that expressed both D1

Discussion and Conclusions

EAAC1 is present in much lower concentrations than other glutamate transporters such as GLAST and GLT-1 in the mammalian brain (Holmseth et al., 2012). Therefore, it is not the most widely studied glutamate transporter, and its role in CNS signaling is largely unknown. The highest concentration of EAAC1 is present in the hippocampus, where EAAC1 prolongs glutamate clearance by astrocytes (Scimemi et al., 2009). However, EAAC1 is also candidate gene for OCD, which develops from deficiencies in the striatum (Samuels et al., 2011), where it is much less abundant and its contribution to the etiology of OCD is contested. Thus far, it has been shown that EAAC1 modulates mGluRI activation, synaptic plasticity, and D1 receptor activation in excitatory circuits of the striatum (Bellini et al., 2018). The effect of EAAC1 on inhibitory circuits in the direct (D1) and indirect (D2) pathway and the relationship between them is not well explored, however. Here, we show that EAAC1 modulation on inhibitory circuits is more pronounced in D1-D1 connections. We propose that the differential effect of EAAC1 at striatal connections may be due to differential concentrations of EAAC1 at these connections. Previous work has measured the concentration of EAAC1 in different regions of the brain (Holmseth et al., 2012), however none to our knowledge have measured EAAC1 concentration in D1 and D2 circuits within a region of the brain such as the striatum.

The fact that TBOA reduces mIPSC amplitude in D1-, but not D2-MSNs (**Figure 1**) shows that EAAC1 may play a greater role at inhibitory synapses onto D1-MSNs, and a far less significant role in inhibition of D2-MSNs. Since TBOA may block other glutamate transporters in addition to EAAC1, such as GLAST and GLT-1, some of this decreased amplitude of mIPSCs in D1-MSNs may be due to blockade of these transporters, in addition to EAAC1. However, when EAAC1 is knocked out with the insertion of a neomycin cassette into the EAAC1 gene, TBOA

does not reduce the amplitude of mIPSCs in both D1- and D2-MSNs (**Figure 2**) meaning that all the reduction in amplitude of mIPSCs in D1-MSNs of WT mice must be due to the effects of EAAC1, and not GLAST or GLT-1.

We were able to achieve effective transfection of Chr2 into the striatum (**Figure 3**). When we examined the specific relationships between D1 and D2-MSNs in WT and EAAC1^{-/-} mice, the absence of EAAC1 decreased evoked IPSC amplitude in D1-D1 connections but did not decrease evoked IPSC amplitude in any other connection (D1-D2, D2-D1, and D2-D2) (**Figure 4**). A D1-MSN in an WT mouse may be more susceptible to GABA release from D1-MSNs, compared to other sources (**Figure 5**). We believe that when EAAC1 is missing, the transport of glutamate into presynaptic terminals is impaired. Since glutamate serves as a metabolic precursor for the synthesis of GABA, an absence of EAAC1 would also impair a presynaptic neuron's ability to synthesize GABA. This leads to a decrease in GABA release from the presynaptic terminal and the observed decrease in the amplitude of IPSCs in the D1-MSNs that we recorded from (Matthews & Diamond, 2003). This may have implications in the lack of inhibition of behaviors seen in OCD patients.

The lack of TBOA sensitivity of non D1-D1 inputs indicates that here, EAAC1 is either not expressed or not able to modulate inhibitory transmission. This may be due to a difference of expression and density of EAAC1 glutamate transporters at D1-D1 synapses and non D1-D1 synapses (e.g., D1-D2, D2-D1, and D2-D2). This difference in expression can be detected by RNAscope FISH (Wang et al., 2012), which we use to determine the concentration of EAAC1 mRNA in D1- and D2-MSNs (**Figure 6**).

We found that there is a more significant cluster of MSNs that express both D1 dopamine receptors and EAAC1, as opposed to MSNs that express both D2 receptors and EAAC1 (**Figure 7**), showing that EAAC1 may be more concentrated at D1-D1 synapses. This reveals that the

preferential effect of EAAC1 at D1-D1 synapses may be due to an increased concentration of glutamate transporter EAAC1 at these synapses. However, most MSNs fell into clusters that either expressed all three mRNAs (D1, D2, and EAAC1) or none of them. This calls into question the accuracy and precision of the RNAscope. A great deal of MSNs stained by DAPI did not receive any puncta from the RNAscope, while a great deal received all three probes, hinting at a possibility of lack of penetration of the probes or unspecific binding in each case. Setting proper thresholds for identification of MSNs and puncta may also pose a problem for future studies using RNAscope to measure mRNA concentration.

Studies into the etiology of OCD have long found serotonergic and dopaminergic systems to be involved. N-acetylcysteine (NAC) has been found to reduce serotonin 1B receptor agonist deficits and OCD-like behavior in mice, which was present at 3 weeks, but not 1 week after treatment (Allen et al., 2018). NAC has also been indicated as a possible treatment for Parkinson's Disease, a result of reduced ability to uptake cysteine by dopaminergic neurons in the substantia nigra of EAAC1^{-/-} mice (Berman et al., 2011). As our understanding of cell signaling pathways in the brain increases, the widespread effects of drugs on multiple pathways becomes more thoroughly understood, as NAC has effects on both dopaminergic and serotonergic pathways.

Selective serotonin reuptake inhibitors as well as cognitive behavioral therapy have been used to treat OCD thus far. The insight that we provide into the role of EAAC1 and dopamine signaling in OCD could potentially lead to a more robust pharmacology involving control of the activity of EAAC1, or modulation of D1 and D2 striatal circuits to treat OCD patients. Understanding the interplay between the excitatory and inhibitory circuits as well as the direct and indirect pathways of the striatum will help us gain a greater insight into the pathology of OCD and how best to treat it.

References

- Allen, E. M., Hughes, E. F., Anderson, C. J., & Woehrle, N. S. (2018). N-acetylcysteine blocks serotonin 1B agonist-induced OCD-related behavior in mice. *Behavioral Neuroscience*, 132(4), 258-268. <https://doi.org/10.1037/bne0000251>
- Báez-Mendoza, R., & Schultz, W. (2013). The role of the striatum in social behavior. *Frontiers in Neuroscience*, 7, 233. <https://doi.org/10.3389/fnins.2013.00233>
- Bellini, S., Fleming, K. E., De, M., McCauley, J. P., Petroccione, M. A., D'Brant, L. Y., Tkachenko, A., Kwon, S., Jones, L. A., & Scimemi, A. (2018). Neuronal glutamate transporters control dopaminergic signaling and compulsive behaviors. *The Journal of Neuroscience*, 38(4), 937–961. <https://doi.org/10.1523/JNEUROSCI.1906-17.2017>
- Berman, A. E., Chan, W. Y., Brennan, A. M., Reyes, R. C., Adler, B. L., Suh, S. W., Kauppinen, T. M., Edling, Y., & Swanson, R. A. (2011). N-acetylcysteine prevents loss of dopaminergic neurons in the EAAC1^{-/-} mouse. *Annals of Neurology*, 69(3), 509–520. <https://doi.org/10.1002/ana.22162>
- Freeze, B. S., Kravitz, A. V., Hammack, N., Berke, J. D., & Kreitzer, A. C. (2013). Control of Basal Ganglia Output by Direct and Indirect Pathway Projection Neurons. *The Journal of Neuroscience*, 33(47), 18531-18539. <https://doi.org/10.1523/JNEUROSCI.1278-13.2013>
- He, Y., Janssen, W. G. M., Rothstein, J. D. & Morrison, J. H. (2000). Differential synaptic localization of the glutamate transporter EAAC1 and glutamate receptor subunit GluR2 in the rat hippocampus. *Journal of Comparative Neurology*, 418(3), 255– 269. [https://doi.org/10.1002/\(SICI\)1096-9861\(20000313\)418:3<255::AID-CNE2>3.0.CO;2-6](https://doi.org/10.1002/(SICI)1096-9861(20000313)418:3<255::AID-CNE2>3.0.CO;2-6)

- Holmseth, S., Dehnes, Y., Huang, Y. H., Follin-Arbelet, V. V., Grutle, N. J., Mylonakou, M. N., Plachez, C., Zhou, Y., Furness, D. N., Bergles, D. E., Lehre, K. P., & Danbolt, N. C. (2012). The density of EAAC1 (EAAT3) glutamate transporters expressed by neurons in the mammalian CNS. *The Journal of Neuroscience*, 32(17), 6000–6013. <https://doi.org/10.1523/JNEUROSCI.5347-11.2012>
- Jenike, M. A. (2004). Obsessive–compulsive disorder. *The New England Journal of Medicine*, 350, 259-265. <https://doi.org/10.1056/NEJMcp031002>
- Kim, H., Kim, M., Im, S. K., & Fang, S. (2018). Mouse Cre-LoxP system: General principles to determine tissue-specific roles of target genes. *Laboratory Animal Research*, 34(4), 147–159. <https://doi.org/10.5625/lar.2018.34.4.147>
- Mathews, G. C., & Diamond, J. S. (2003). Neuronal glutamate uptake Contributes to GABA synthesis and inhibitory synaptic strength. *The Journal of Neuroscience*, 23(6), 2040-2048. <https://doi.org/10.1523/JNEUROSCI.23-06-02040.2003>
- Nagel, G., Szellas, T., Huhn, W., Keteriya, S., Adeishvili, N., Berthold, P., Ollig, D., Hegemann, P., & Bamberg, E. (2003). Channelrhodopsin-2, a directly light-gated cation-selective membrane channel. *Proceedings of the National Academy of the United States of America*, 100(24), 13940-13945. <https://doi.org/10.1073/pnas.1936192100>
- Purty, A., Nestadt, G., Samuels, J. F., & Viswanath, B. (2019). Genetics of obsessive-compulsive disorder. *Indian Journal of Psychiatry*, 61(Suppl 1), S37–S42. https://doi.org/10.4103/psychiatry.IndianJPsychiatry_518_18

- Rothstein, J. D., Martin, L., Levey, A. I., Dykes-Hoberg, M., Jin, L., Wu, D., Nash, N., & Kuncel, R. W. (1994). Localization of neuronal and glial glutamate transporters. *Neuron*, *13*(3), 713–725. [https://doi.org/10.1016/0896-6273\(94\)90038-8](https://doi.org/10.1016/0896-6273(94)90038-8)
- Samuels, J., Wang, Y., Riddle, M. A., Greenberg, B. D., Fyer, A. J., McCracken, J. T., Rauch, S. L., Murphy, D. L., Grados, M. A., Knowles, J. A., Piacentini, J., Cullen, B., Bienvenu, O. J 3rd., Rasmussen, S. A., Geller, D., Pauls, D. L., Liang, K. Y., Shugart, Y. Y., & Nestadt, G. (2011). Comprehensive family-based association study of the glutamate transporter gene SLC1A1 in obsessive-compulsive disorder. *American Journal of Medical Genetics Part B: Neuropsychiatric Genetics*, *156B*(4), 472–477. <https://doi.org/10.1002/ajmg.b.31184>
- Scimemi, A., Tian, H., & Diamond, J.S. (2009). Neuronal transporters regulate glutamate clearance, NMDA receptor activation, and synaptic plasticity in the hippocampus. *The Journal of Neuroscience*, *29*(46), 14581-14595. <https://doi.org/10.1523/JNEUROSCI.4845-09.2009>
- Wang, F., Flanagan, J., Su, N., Wang, L. C., Bui, S., Nielson, A., Wu, X., Vo, H. T., Ma, X. J., & Luo, Y. (2012). RNAscope: A novel in situ RNA analysis platform for formalin-fixed, paraffin-embedded tissues. *The Journal of Molecular Diagnostics*, *14*(1), 22–29. <https://doi.org/10.1016/j.jmoldx.2011.08.002>
- Young, C. B., Reddy, V., & Sonne, J. (2020). Neuroanatomy, basal anglia. *StatPearls*. StatPearls Publishing. Retrieved January 2019 from <https://www.ncbi.nlm.nih.gov/books/NBK537141/>